

Nanoindentations on Conch Shells of Gastropoda and Bivalvia Molluscs Reveal Anisotropic Evolution Against External Attacks

Cristina Bignardi^{1,*}, Michele Petraroli¹, and Nicola M. Pugno^{2,3}

¹Department of Mechanics, Politecnico di Torino, Corso Duca degli Abruzzi 24, 10129, Torino, Italy

²Department of Structural Mechanics, Politecnico di Torino, Corso Duca degli Abruzzi 24, 10129, Torino, Italy

³National Institute of Nuclear Physics—National Laboratories of Frascati, via E. Fermi 40, 00044, Frascati, Italy

Nanoindentation method has been used to explore, at the nanoscale, the mechanical properties of four different representative types of conch shells belonging to the two biggest classes of molluscs, Gastropoda and Bivalvia, in order to compare nanohardness and Young's modulus with respect to the microstructural anisotropic architectures. For the experimental tests a Nano Indenter XP (MTS Nano Instruments, Oak Ridge TN) has been used. The mechanical tests have been carried out on the inner and outer surfaces of the shells, as well as on their cross-section, near to the inner/outer surfaces and in the middle layer. The results confirm the three layered anisotropic architecture of the investigated conchs. On each of these 5 surfaces, 2×5 indentations have been performed at different maximum depth: from 250 nm to 4 μm , with a step of 250 nm, for a total of 3200 tests. The numerous observations have been analysed applying an *ad hoc* modification of the Weibull Statistics, suggesting a natural evolution of the shells against external attacks.

Keywords: Nanoindentation, Conch Shell, Nanohardness, Young's Modulus, Weibull.

1. INTRODUCTION

Growth and self-strengthening of natural materials is very attractive. According to Darwin (the year 2009 is the 150th anniversary of the publication of *On the Origin of Species* (November 24th, 1859) and the 200th anniversary of Darwin's birth (February 12th, 1809)), the reason for the survival of living organisms is that they could evolve and improve themselves in such a way to be always compatible with the environment (even if humans seem to be radically different, modifying the environment rather than themselves). Therefore, in such a sense, it is no doubt that natural materials are the most optimized materials in the world. Their hard structures are highly integrated in soft tissues as in natural organisms, as for bone, tooth, mollusc shell, bark, etc. The laminated organization of these structures is inherent at different spatial scales (nano, micro, meso, macro). They all exhibit special properties and functions. From the view-point of the material scientist, it is beneficial to learn from these natural materials and structures and learning from Nature has become now one of the most fascinating subjects in material research.

The majority of shell-forming marine molluscs belong to two main classes: Gastropoda (univalves, or snails) and Bivalvia (bivalves, including clams, oysters, and scallops). Sea shells are composed of calcium carbonate crystals interleaved with layers of viscoelastic proteins, having dense, tailored structures that yield excellent mechanical properties.^{1,2} Shells have architectures that differ depending on growth requirements and shell formation of the particular mollusc.

Conch shells have a cross-lamellar structure that consists of lath-like aragonite crystals (99.9 wt%) and a tenuous organic layer (0.1 wt%).³ The architecture of conch shell is organized in three macro-layers.⁴ Each macro-layer consists of many crossed first-order lamellae, each of them composed by second-order lamellae. Furthermore, the second-order lamella is made up of third-order lamellae, which are considered single-crystals and multicrystals. Further analysis indicates that each lamella is connected to its neighbour lamellae by a proteinaceous adhesive. The first-order lamellae have thickness of 5–30 μm and are several micrometers wide, while the second-order ones are about 5 μm thick and 5–30 μm wide; the third order lamellae are nanosized. Thus, the thickness of the lamellae varies to some extents. In some zones lamellae become

*Author to whom correspondence should be addressed.

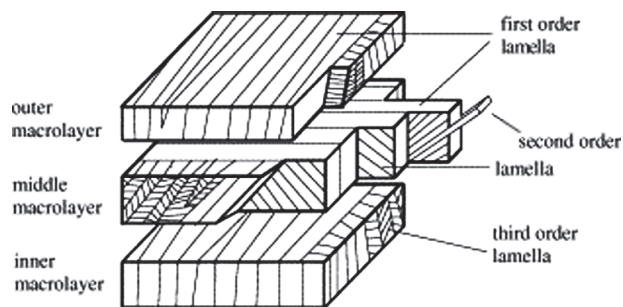


Fig. 1. Schematic diagram of crossed-lamellar three layered anisotropic architecture of conch shell.

rather thinner or eventually disappear. Each lamella consists of lath-like crystals. The hierarchical lamellae have different orientations. Moreover, the lamellae are rotated in the “lamellar plane” of an angle about 70–90° with respect to their neighbour layer/layers. The complete microscopic plywood sketch map of conch shell is shown in Figure 1.

In this paper we have investigated the nanomechanical anisotropic properties of the shells with a nanoindenter, making 3200 tests, then treated with an *ah hoc* modification of the Weibull Statistics.

2. NANOINDENTATION EXPERIMENTS

Nanoindentation method has been used to explore, at the nanoscale, the mechanical properties of four different representative types of conch shells belonging to the two biggest classes of molluscs, Gastropoda and Bivalvia, in order to compare nanohardness and Young’s modulus with respect to the microstructural anisotropic architecture. The conch shells chosen are: *Pecten jacobaeus* (Linnaeus, 1758),⁵ *Pinna nobilis* (Linnaeus, 1758), *Venus verrucosa* (Linnaeus, 1758) and *Conus mediterraneus* (Hwass, 1792),⁶ Figure 2.

For the experimental tests a Nano Indenter XP (MTS Nano Instruments, Oak Ridge TN) has been used. The mechanical tests have been carried out on the inner/outer surfaces of each shell and on three zones along their cross section (inner, middle and outer) in order to determine the nanohardness and Young’s modulus by varying position and orientation, Figure 3. Specimens were incorporated inside a resin support, Figure 4, and those of the

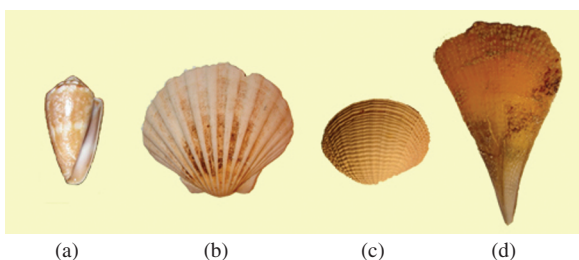


Fig. 2. (a) *Conus mediterraneus* conch, (b) *Pecten jacobaeus* conch, (c) *Venus verrucosa* conch and (d) *Pinna nobilis* conch.

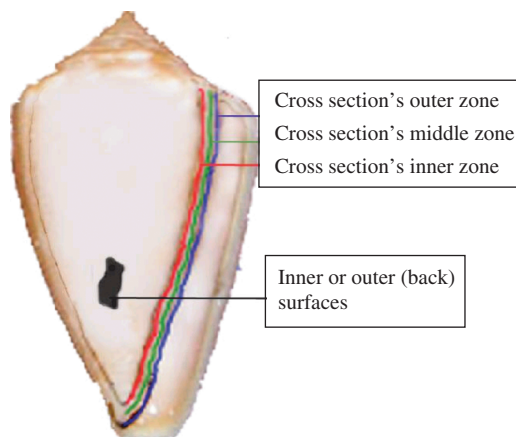


Fig. 3. Example of indentation zones on *Conus mediterraneus* conch.

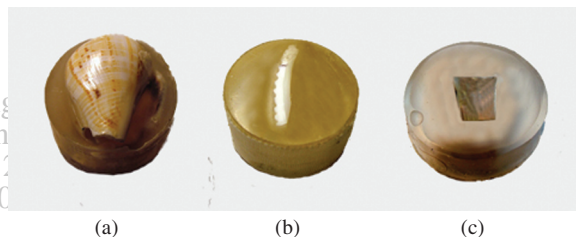


Fig. 4. Some of the specimens used: (a) outer surface of the *Conus mediterraneus* conch shell, (b) cross section zones of the *Venus verrucosa* conch shell, (c) inner surface of the *Pinna nobilis* conch shell.

cross-section have been lapped in order to obtain a flat surface. On each of these surfaces the indentation has been performed at different maximum depth: from 250 nm to 4 μm, with a step of 250 nm. Both on the inner/outer surfaces and on each cross-sectional zone every test consisted of an indentation matrix 2 × 5: thus globally 3200 indentations have been performed, 800 for each conch shell. In the choice of the area to indent it has been taken care to avoid the nanoindentation-boundary interaction and, for each matrix, the distance between the indentation points has been increased by increasing the indentation depth, in order to avoid their self-interactions too.

The Oliver-Pharr model was used for data extraction.⁷ According to this method, a loading–unloading cycle is applied and the maximum force measured, averaged on the corresponding indentation area, gives the nanohardness of the specimen, while from the slope of the unloading curve its Young’s modulus can be derived. Each indentation was made using a diamond Berkovich tip.

3. STATISTICAL DATA TREATMENT

Results obtained for nanohardness are reported in Table I and Figure 5 or for Young’s modulus in Table II and Figure 6. Each table or Figure is related to one of the five surfaces tested and shows nanohardness or Young’s modulus at 16 different depths. Each data reported in Tables I, II

Table I(a)–(e). (a) Nanohardness measurements on the inner surface, (b) Nanohardness measurements on the cross section inner zone, (c) Nanohardness measurements on the cross section middle zone, (d) Nanohardness measurements on the cross section outer zone, (e) Nanohardness measurements on the outer surface.

Depth [nm]	CM	PJ	VV	PN
(a) Inner surface-Nanohardness [GPa]				
250	2.960 ± 1.938	6.648 ± 6.060	2.983 ± 3.530	1.612 ± 1.608
500	2.355 ± 1.828	1.470 ± 1.754	3.901 ± 3.226	2.258 ± 1.894
750	2.715 ± 1.110	2.167 ± 2.548	2.878 ± 2.214	2.657 ± 3.010
1000	2.466 ± 0.612	1.806 ± 1.654	2.449 ± 1.748	2.383 ± 1.566
1250	2.813 ± 0.762	1.238 ± 1.908	2.215 ± 1.396	2.491 ± 1.126
1500	1.549 ± 1.678	2.759 ± 0.888	2.556 ± 2.140	2.010 ± 1.618
1750	1.456 ± 2.204	2.587 ± 2.040	2.669 ± 2.056	2.119 ± 1.074
2000	2.631 ± 0.406	2.938 ± 0.624	3.289 ± 1.542	2.482 ± 1.030
2250	2.067 ± 2.530	2.795 ± 0.792	3.352 ± 1.616	2.384 ± 0.786
2500	2.766 ± 0.760	2.655 ± 0.514	3.299 ± 1.510	2.144 ± 0.710
2750	2.443 ± 1.028	1.333 ± 1.806	2.691 ± 2.656	2.415 ± 1.262
3000	2.208 ± 1.360	0.719 ± 1.458	3.363 ± 1.764	2.488 ± 0.886
3250	2.642 ± 1.278	1.647 ± 1.678	3.355 ± 1.432	2.411 ± 0.734
3500	2.366 ± 1.838	1.722 ± 1.874	3.097 ± 1.852	2.256 ± 0.824
3750	2.431 ± 1.280	2.421 ± 0.568	2.789 ± 2.566	2.615 ± 0.642
4000	3.064 ± 1.292	2.321 ± 0.926	3.335 ± 0.862	2.858 ± 0.788
(b) Cross section inner zone-Nanohardness [GPa]				
250	0.225 ± 0.044	0.736 ± 1.050	0.302 ± 0.440	0.080 ± 0.242
500	0.140 ± 0.096	1.073 ± 1.468	0.253 ± 0.152	0.440 ± 1.132
750	0.105 ± 0.066	1.086 ± 1.602	0.216 ± 0.110	0.419 ± 0.548
1000	0.118 ± 0.106	0.785 ± 0.478	0.203 ± 0.106	0.580 ± 0.582
1250	0.097 ± 0.034	1.030 ± 0.612	0.217 ± 0.110	0.629 ± 0.666
1500	0.061 ± 0.032	0.977 ± 0.672	0.218 ± 0.100	0.602 ± 0.876
1750	0.096 ± 0.036	1.132 ± 0.360	0.230 ± 0.074	0.601 ± 0.610
2000	0.080 ± 0.044	0.825 ± 0.468	0.240 ± 0.076	0.570 ± 0.614
2250	0.074 ± 0.036	0.737 ± 0.266	0.189 ± 0.054	0.722 ± 0.560
2500	0.085 ± 0.048	0.804 ± 0.310	0.215 ± 0.064	1.016 ± 0.614
2750	0.082 ± 0.038	0.759 ± 0.302	0.221 ± 0.062	1.220 ± 0.456
3000	0.068 ± 0.030	0.632 ± 0.190	0.220 ± 0.066	1.499 ± 0.694
3250	0.071 ± 0.034	0.674 ± 0.330	0.325 ± 0.256	1.334 ± 0.888
3500	0.073 ± 0.020	0.655 ± 0.544	0.205 ± 0.036	0.877 ± 1.070
3750	0.071 ± 0.022	0.584 ± 0.440	0.223 ± 0.044	1.111 ± 0.864
4000	0.060 ± 0.024	0.652 ± 0.246	0.201 ± 0.064	1.086 ± 0.722
(c) Cross section middle zone-Nanohardness [GPa]				
250	2.308 ± 2.458	2.413 ± 2.222	2.023 ± 3.482	1.301 ± 2.022
500	2.045 ± 1.236	2.580 ± 1.970	3.600 ± 1.594	1.029 ± 1.914
750	3.178 ± 1.376	3.889 ± 3.012	4.001 ± 1.938	1.275 ± 1.816
1000	3.786 ± 2.900	3.936 ± 1.872	3.940 ± 2.350	2.794 ± 1.664
1250	3.520 ± 1.878	3.879 ± 1.636	2.842 ± 1.892	2.503 ± 1.770
1500	3.090 ± 2.320	3.892 ± 1.112	2.851 ± 1.056	2.702 ± 1.828
1750	3.587 ± 0.996	4.008 ± 1.096	1.817 ± 1.734	2.739 ± 0.948
2000	3.610 ± 2.276	3.964 ± 1.060	2.984 ± 1.752	2.975 ± 0.846
2250	3.664 ± 1.538	3.799 ± 0.716	1.673 ± 1.742	2.702 ± 0.534
2500	3.253 ± 0.554	4.142 ± 1.072	2.281 ± 1.912	1.802 ± 1.366
2750	3.691 ± 1.594	3.683 ± 0.720	2.794 ± 1.122	2.002 ± 0.702
3000	3.590 ± 0.860	3.921 ± 0.708	2.621 ± 0.814	1.799 ± 0.408
3250	3.823 ± 0.482	3.872 ± 0.894	1.370 ± 1.548	1.935 ± 1.172
3500	3.676 ± 0.718	3.438 ± 0.588	1.931 ± 1.230	1.881 ± 0.540
3750	3.675 ± 0.664	3.850 ± 0.766	2.646 ± 1.230	1.620 ± 0.732
4000	3.551 ± 0.986	3.839 ± 1.262	2.747 ± 1.024	1.789 ± 0.598
(d) Cross section outer zone-Nanohardness [GPa]				
250	1.891 ± 1.664	0.308 ± 0.136	3.623 ± 2.564	1.020 ± 1.192
500	2.005 ± 1.944	1.028 ± 1.392	3.212 ± 2.672	1.118 ± 1.504
750	2.461 ± 1.862	1.599 ± 0.898	3.205 ± 1.490	0.347 ± 0.292
1000	2.922 ± 1.382	2.149 ± 1.470	3.199 ± 1.576	0.303 ± 0.676
1250	1.863 ± 1.978	1.893 ± 1.338	3.543 ± 0.504	1.015 ± 1.388
1500	2.947 ± 0.784	2.289 ± 0.956	3.341 ± 0.558	1.021 ± 1.478
1750	2.924 ± 2.816	1.269 ± 1.282	2.976 ± 1.188	0.590 ± 0.680

Continued.

Table I(a)–(e). Continued.

Depth [nm]	CM	PJ	VV	PN
2000	3.344 ± 0.830	1.065 ± 1.508	2.872 ± 1.386	0.834 ± 0.786
2250	4.000 ± 0.822	1.011 ± 0.900	3.292 ± 1.098	0.905 ± 0.930
2500	4.257 ± 1.084	0.612 ± 0.772	2.945 ± 1.072	1.079 ± 0.812
2750	3.422 ± 1.126	1.114 ± 0.620	3.095 ± 1.096	0.476 ± 0.300
3000	2.837 ± 0.838	1.026 ± 0.516	2.998 ± 0.856	0.821 ± 1.086
3250	3.846 ± 1.288	0.818 ± 1.266	2.224 ± 2.254	0.015 ± 0.026
3500	3.332 ± 1.212	0.781 ± 1.056	1.295 ± 1.794	0.371 ± 0.598
3750	3.395 ± 0.940	0.903 ± 0.926	0.490 ± 0.490	0.221 ± 0.188
4000	2.893 ± 0.442	0.366 ± 0.402	0.497 ± 0.448	0.200 ± 0.152

(e) Outer surface-Nanohardness [GPa]	CM	PJ	VV	PN
250	4.585 ± 3.238	1.586 ± 3.270	1.492 ± 2.174	3.880 ± 0.540
500	4.198 ± 3.616	0.877 ± 1.236	0.894 ± 0.534	3.398 ± 1.240
750	4.471 ± 2.134	0.362 ± 0.560	0.783 ± 0.612	3.669 ± 1.478
1000	4.473 ± 2.740	0.567 ± 0.676	0.575 ± 0.286	2.576 ± 1.466
1250	3.043 ± 3.058	0.898 ± 0.710	0.498 ± 0.188	2.666 ± 1.422
1500	4.485 ± 1.770	0.707 ± 0.972	0.492 ± 0.228	2.938 ± 1.624
1750	4.635 ± 0.742	0.578 ± 1.018	0.374 ± 0.212	2.156 ± 1.152
2000	4.043 ± 3.270	0.420 ± 0.656	0.504 ± 0.106	0.777 ± 0.912
2250	3.926 ± 2.394	0.745 ± 1.170	0.472 ± 0.204	2.334 ± 1.222
2500	3.940 ± 3.792	0.857 ± 0.968	0.433 ± 0.126	2.119 ± 0.638
2750	3.992 ± 1.368	0.518 ± 1.002	0.442 ± 0.336	2.085 ± 1.418
3000	3.652 ± 1.678	1.592 ± 1.590	0.646 ± 0.674	1.671 ± 1.620
3250	4.296 ± 2.304	0.665 ± 0.908	1.121 ± 0.844	1.241 ± 1.470
3500	3.418 ± 1.926	0.869 ± 1.102	1.229 ± 1.246	0.427 ± 0.426
3750	3.334 ± 2.788	0.592 ± 0.812	0.658 ± 0.646	0.533 ± 1.254
4000	3.557 ± 2.474	1.178 ± 1.404	0.627 ± 0.668	0.346 ± 0.336

Matrix mean values and standard deviations; (CM) Conus Mediterraneus, (PJ) Pecten Jacobeus, (VV) Venus Verrucosa, (PN) Pinna Nobilis.

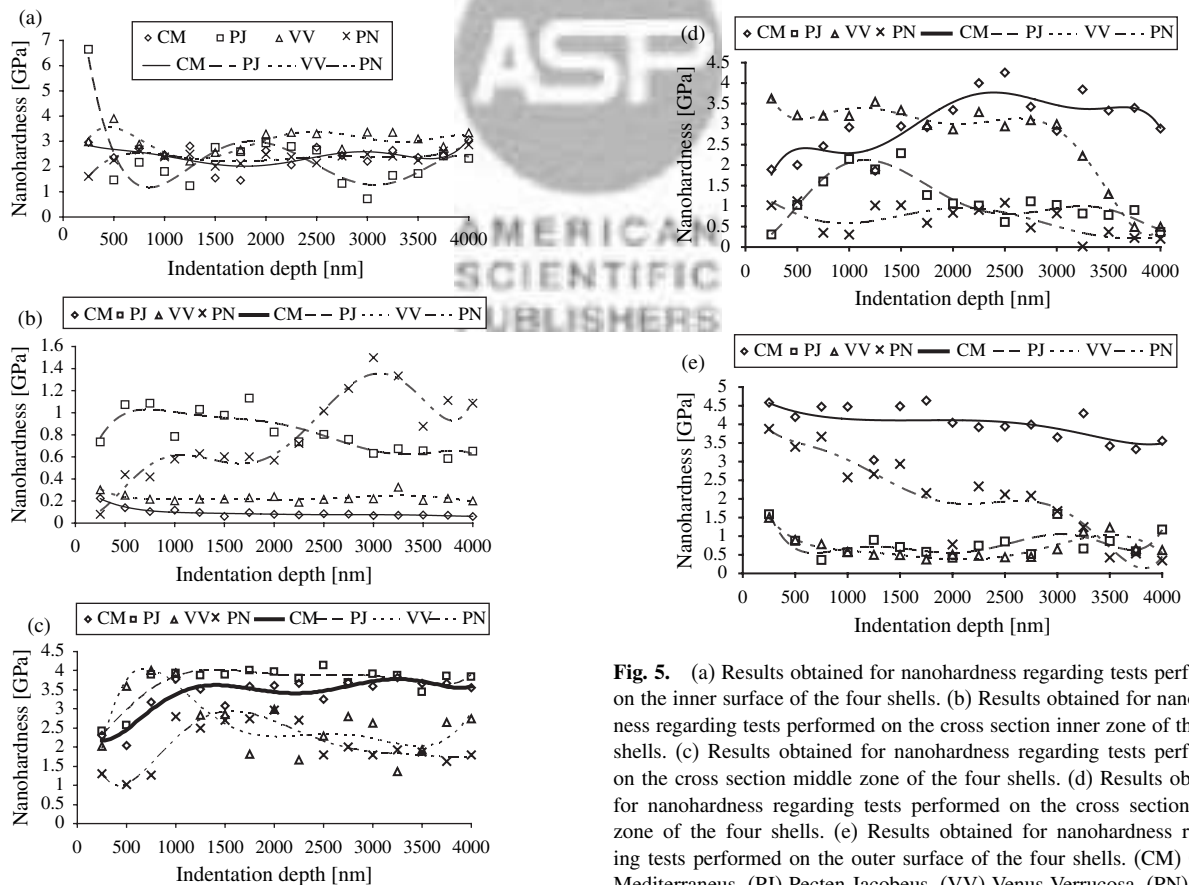


Fig. 5. (a) Results obtained for nanohardness regarding tests performed on the inner surface of the four shells. (b) Results obtained for nanohardness regarding tests performed on the cross section inner zone of the four shells. (c) Results obtained for nanohardness regarding tests performed on the cross section middle zone of the four shells. (d) Results obtained for nanohardness regarding tests performed on the cross section outer zone of the four shells. (e) Results obtained for nanohardness regarding tests performed on the outer surface of the four shells. (CM) Conus Mediterraneus, (PJ) Pecten Jacobeus, (VV) Venus Verrucosa, (PN) Pinna Nobilis.

Fig. 5. Continued.

Table II(a)–(e). (a) Young's modulus measurements on the inner surface, (b) Young's modulus measurements on the cross section inner zone, (c) Young's modulus measurements on the cross section middle zone, (d) Young's modulus measurements on the cross section outer zone, (e) Young's modulus measurements on the outer surface.

Depth [nm]	CM	PJ	VV	PN
(a) Inner surface–Young's modulus [GPa]				
250	81.279 ± 17.816	158.140 ± 41.988	76.077 ± 46.928	43.722 ± 25.560
500	74.370 ± 18.576	63.099 ± 32.914	102.189 ± 47.702	51.170 ± 22.662
750	72.426 ± 10.712	70.070 ± 29.798	83.247 ± 38.488	49.904 ± 27.248
1000	68.667 ± 7.910	68.301 ± 24.380	74.024 ± 18.026	44.490 ± 13.096
1250	70.714 ± 6.768	54.039 ± 43.578	74.393 ± 21.308	42.212 ± 8.114
1500	52.981 ± 32.346	75.782 ± 8.228	76.652 ± 23.400	37.870 ± 11.072
1750	49.288 ± 29.130	70.110 ± 36.068	76.038 ± 21.730	37.314 ± 7.824
2000	63.450 ± 2.448	73.509 ± 6.724	88.814 ± 19.330	38.703 ± 5.352
2250	52.015 ± 34.358	71.831 ± 9.854	85.201 ± 20.594	37.627 ± 4.486
2500	59.701 ± 5.894	69.745 ± 6.844	84.908 ± 19.012	36.027 ± 4.814
2750	56.869 ± 13.532	51.203 ± 34.800	73.265 ± 34.562	36.980 ± 8.294
3000	55.101 ± 12.122	45.240 ± 29.758	79.923 ± 18.584	38.371 ± 4.800
3250	60.612 ± 12.366	54.518 ± 25.204	76.997 ± 10.844	37.617 ± 4.512
3500	54.667 ± 13.148	57.345 ± 27.006	76.154 ± 17.686	38.309 ± 3.514
3750	55.266 ± 12.908	63.713 ± 6.658	73.751 ± 39.782	39.307 ± 3.922
4000	60.041 ± 8.536	62.636 ± 11.576	73.211 ± 11.726	41.351 ± 4.806
(b) Cross section inner zone–Young's modulus [GPa]				
250	1.148 ± 0.370	36.575 ± 40.406	4.984 ± 3.260	1.130 ± 2.282
500	0.811 ± 0.168	42.990 ± 38.016	4.741 ± 1.862	26.457 ± 38.744
750	0.616 ± 0.136	40.620 ± 39.684	4.608 ± 1.456	19.404 ± 25.656
1000	0.553 ± 0.208	34.607 ± 19.128	4.315 ± 1.474	26.832 ± 17.726
1250	0.461 ± 0.070	39.035 ± 11.178	4.717 ± 1.464	27.574 ± 8.340
1500	0.352 ± 0.084	39.460 ± 14.116	4.629 ± 0.946	23.686 ± 22.884
1750	0.377 ± 0.054	41.777 ± 13.302	4.816 ± 0.982	24.590 ± 17.436
2000	0.325 ± 0.086	36.470 ± 12.830	5.445 ± 3.578	23.728 ± 16.082
2250	0.309 ± 0.050	32.501 ± 3.210	4.231 ± 0.766	30.475 ± 10.498
2500	0.288 ± 0.092	34.194 ± 4.866	4.440 ± 0.956	40.052 ± 12.874
2750	0.260 ± 0.076	33.637 ± 4.934	4.649 ± 0.972	42.492 ± 11.490
3000	0.240 ± 0.060	32.064 ± 8.040	4.519 ± 0.748	47.624 ± 10.422
3250	0.235 ± 0.066	30.021 ± 9.272	11.864 ± 20.064	44.846 ± 10.520
3500	0.235 ± 0.052	33.249 ± 19.940	4.266 ± 0.426	36.853 ± 22.002
3750	0.222 ± 0.058	30.588 ± 12.498	4.424 ± 0.612	41.776 ± 15.250
4000	0.212 ± 0.042	29.249 ± 8.166	4.118 ± 0.662	39.905 ± 10.018
(c) Cross section middle zone–Young's modulus [GPa]				
250	71.655 ± 48.894	81.889 ± 40.584	54.291 ± 58.910	40.942 ± 42.484
500	71.315 ± 27.448	78.443 ± 28.356	76.019 ± 22.378	36.495 ± 45.432
750	74.650 ± 14.360	88.513 ± 31.648	71.383 ± 11.840	47.723 ± 35.810
1000	78.856 ± 28.222	85.835 ± 21.426	65.405 ± 15.322	74.669 ± 23.928
1250	73.304 ± 20.580	83.654 ± 16.882	53.780 ± 11.834	70.897 ± 28.232
1500	61.911 ± 25.920	80.019 ± 12.346	49.263 ± 5.284	71.225 ± 25.502
1750	71.338 ± 9.928	81.225 ± 13.060	42.051 ± 9.480	71.729 ± 14.944
2000	71.174 ± 22.840	77.939 ± 11.126	46.813 ± 7.454	75.633 ± 15.152
2250	71.822 ± 14.384	75.745 ± 8.120	34.226 ± 16.398	69.159 ± 8.016
2500	65.045 ± 6.768	77.914 ± 15.054	41.678 ± 10.780	60.981 ± 27.492
2750	69.830 ± 13.836	73.380 ± 6.586	42.704 ± 6.046	61.925 ± 9.732
3000	67.038 ± 10.758	74.489 ± 7.376	41.666 ± 4.306	56.636 ± 11.994
3250	66.316 ± 2.820	72.934 ± 9.862	32.498 ± 11.618	61.709 ± 16.006
3500	63.516 ± 6.200	67.930 ± 5.954	35.910 ± 7.720	57.928 ± 10.670
3750	62.770 ± 6.102	72.175 ± 10.096	38.138 ± 5.982	52.967 ± 15.138
4000	62.323 ± 8.710	70.002 ± 8.232	36.956 ± 5.812	53.883 ± 10.218
(d) Cross section outer zone–Young's modulus [GPa]				
250	67.321 ± 32.026	5.135 ± 1.982	71.345 ± 26.300	29.613 ± 33.994
500	64.372 ± 40.712	28.634 ± 35.434	67.633 ± 16.862	45.177 ± 30.642
750	66.923 ± 27.956	45.858 ± 7.546	61.235 ± 15.370	19.371 ± 12.822
1000	72.572 ± 18.380	47.969 ± 19.354	56.635 ± 9.426	20.492 ± 37.794
1250	56.387 ± 27.206	36.296 ± 20.492	53.308 ± 4.172	46.354 ± 33.914
1500	69.231 ± 15.104	38.056 ± 11.456	48.775 ± 1.900	43.150 ± 35.896
1750	68.175 ± 28.194	25.664 ± 16.456	43.905 ± 6.624	33.701 ± 24.802
2000	70.863 ± 10.676	23.729 ± 15.744	60.831 ± 7.902	41.386 ± 20.218

Continued.

Table II(a)–(e). Continued.

Depth [nm]	CM	PJ	VV	PN
2250	67.929 ± 6.502	25.842 ± 14.930	40.776 ± 5.028	46.703 ± 22.028
2500	69.148 ± 8.270	21.603 ± 21.340	38.759 ± 3.532	50.566 ± 18.856
2750	60.788 ± 6.416	38.125 ± 12.594	36.877 ± 3.832	34.328 ± 17.724
3000	62.926 ± 9.312	37.966 ± 12.296	34.495 ± 2.750	42.746 ± 36.060
3250	58.085 ± 8.288	27.762 ± 31.224	28.957 ± 11.436	0.634 ± 1.228
3500	54.617 ± 9.722	22.801 ± 24.670	24.200 ± 9.742	28.779 ± 20.026
3750	52.964 ± 7.564	27.527 ± 22.962	17.267 ± 5.692	15.918 ± 28.586
4000	62.467 ± 4.316	16.159 ± 24.342	16.020 ± 7.052	15.395 ± 15.930
(e) Outer surface–Young’s modulus [GPa]				
250	83.946 ± 36.172	34.904 ± 33.518	26.146 ± 12.810	58.133 ± 8.366
500	75.668 ± 28.860	29.083 ± 32.668	30.066 ± 21.320	50.565 ± 15.452
750	80.058 ± 15.162	21.090 ± 32.514	53.334 ± 37.128	53.672 ± 10.260
1000	79.559 ± 20.274	29.378 ± 42.356	50.011 ± 25.766	45.708 ± 11.602
1250	74.599 ± 46.044	41.159 ± 12.902	37.239 ± 27.864	47.924 ± 12.820
1500	76.422 ± 14.534	42.665 ± 45.442	36.504 ± 19.134	48.023 ± 16.260
1750	76.038 ± 5.328	36.778 ± 43.280	23.134 ± 14.506	42.119 ± 13.480
2000	77.272 ± 23.380	22.735 ± 27.700	39.590 ± 7.578	30.254 ± 16.102
2250	73.014 ± 19.526	47.414 ± 38.834	42.094 ± 14.534	45.706 ± 11.132
2500	75.154 ± 33.076	44.930 ± 30.546	43.432 ± 10.366	41.823 ± 6.718
2750	70.583 ± 10.536	36.824 ± 43.588	45.395 ± 29.766	41.752 ± 14.216
3000	70.721 ± 9.954	52.850 ± 23.208	47.465 ± 31.962	34.445 ± 23.206
3250	73.558 ± 22.002	36.969 ± 30.768	54.583 ± 13.252	27.997 ± 24.180
3500	65.840 ± 13.386	43.234 ± 28.390	57.026 ± 37.038	16.880 ± 12.554
3750	64.727 ± 25.580	38.552 ± 28.978	69.721 ± 38.238	16.070 ± 14.502
4000	65.531 ± 22.600	51.139 ± 35.480	54.157 ± 29.638	16.375 ± 8.452

Matrix mean values and standard deviations; (CM) Conus Mediterraneus, (PJ) Pecten Jacobeus, (VV) Venus Verrucosa, (PN) Pinna Nobilis.

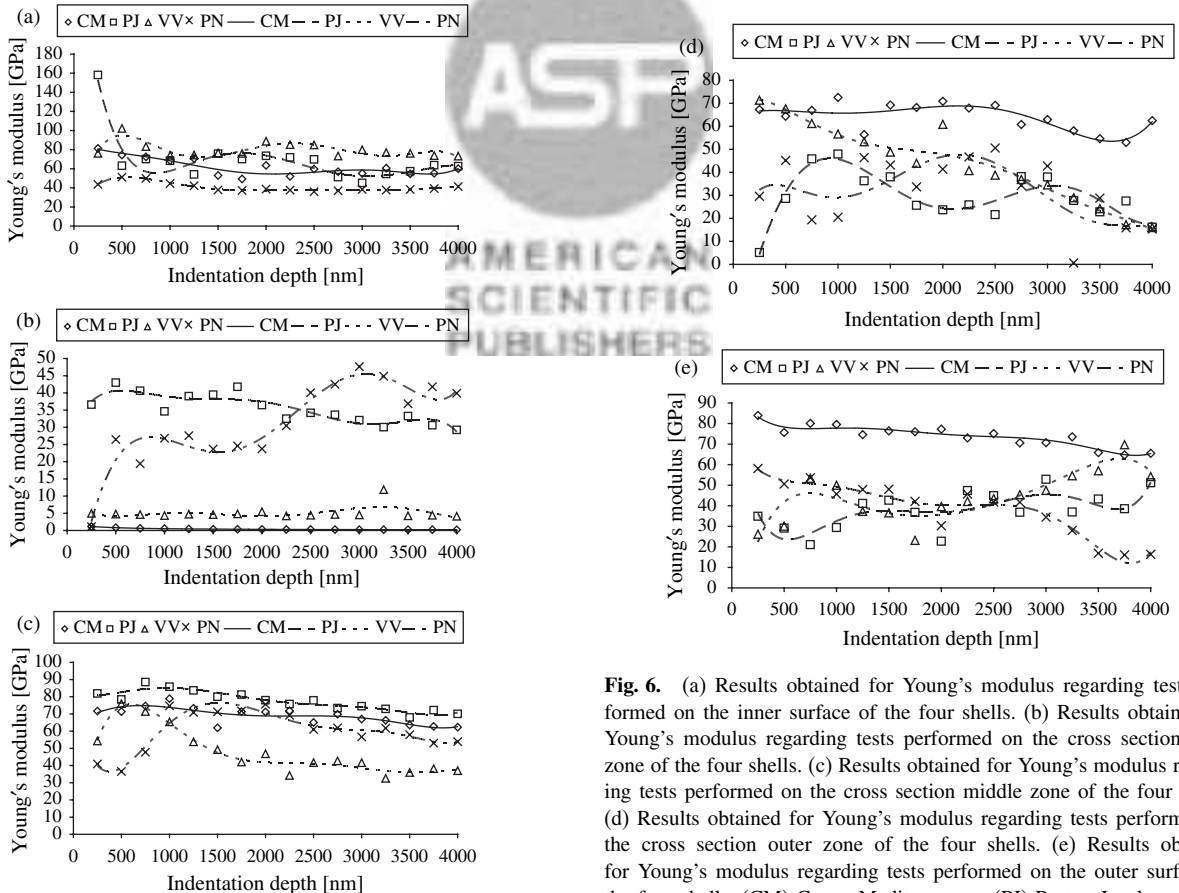


Fig. 6. (a) Results obtained for Young’s modulus regarding tests performed on the inner surface of the four shells. (b) Results obtained for Young’s modulus regarding tests performed on the cross section inner zone of the four shells. (c) Results obtained for Young’s modulus regarding tests performed on the cross section middle zone of the four shells. (d) Results obtained for Young’s modulus regarding tests performed on the cross section outer zone of the four shells. (e) Results obtained for Young’s modulus regarding tests performed on the outer surface of the four shells. (CM) Conus Mediterraneus, (PJ) Pecten Jacobeus, (VV) Venus Verrucosa, (PN) Pinna Nobilis.

Fig. 6. Continued.

or point on Figures 5, 6 represents the average value of the indentation matrix.

The 3200 tests have been analysed applying an *ad hoc* modification of the Weibull Statistics,⁸ i.e., interpreting the cumulative probability function F , of finding zones with nanohardness (Young's modulus) smaller than $H(E)$ at an indentation depth h , according to:

$$F(< H) = 1 - e^{-(h/h_0)^n (H/H_0)^m} \quad (1)$$

where H_0 is the nominal nanohardness (or E_0 is the nominal Young's modulus, i.e., corresponding to $F = 63\%$, for $(h/h_0)^n = 1$), h_0 is a reference indentation depth (e.g., $1 \mu\text{m}$), m is the Weibull modulus and n/m is the size-effect exponent. Classically Weibull Statistics is applied considering H as the material strength, h as a characteristic size defined as the cubic root of the specimen volume (or square root of the specimen surface), and thus $n = 3$ (or $n = 2$) for volume (or surface) predominant defects. Alternatively Nanoscale Weibull Statistics,⁹ specifically developed for nearly defect-free structures, considers $n = 0$. Thus, we note that our modification proposed in Eq. (1) describes, in addition to the nanohardness (Young's modulus) distribution, also the indentation size-effect, in

the form of $H \propto h^{-n/m}$ ($E \propto h^{-n/m}$). Similar results are obtained for the different shells; as an example we focus our attention on the *Conus mediterraneus* conch.¹⁰ In our tests a negligible indentation size-effect has been revealed, thus suggesting $n = 0$, for which in fact the highest statistical correlation (coefficient of correlation R^2) is found. An exception for the softer anisotropic inner layer is observed, for which we found the maximum statistical correlation for $n = 3$, suggesting that the size-effect is governed by volume-dominated process, such as dislocation sliding. In fact $n = 0$ would correspond for the nanohardness data analysis to $R^2(n = 0) = 0.7232$, whereas $R^2(n = 1) = 0.8755$, $R^2(n = 2) = 0.9020$, $R^2(n = 3) = 0.9028$, $R^2(n = 4) = 0.8981$, thus with a maximum for $n = 3$. A similar trend is observed for the Young's modulus. As an example, the Weibull plots for the nanohardness measured along the two considered orthogonal directions of the inner anisotropic layer are shown in Figure 7. We note that the proposed modification of the Weibull Statistics is powerful in treating nanoindentation experiments.

Our analysis supports the idea that super-composites or super-armors could be realized in the near future mimicking nacre,¹¹ with anisotropic and hierarchical architectures composed by hard surfaces and tough volumes, in order to increase the material fracture toughness.¹²⁻¹⁶

4. DISCUSSION AND CONCLUSIONS

We have performed 3200 nanoindentations on four different representative types of conch shells belonging to the two biggest classes of molluscs, Gastropoda and Bivalvia, in order to compare nanohardness and Young's modulus with respect to their microstructural anisotropic architecture. The following considerations can be drawn:

- (i) a strong anisotropy of the inner layer is present in all the four investigated shells: nanohardness and Young's modulus increase by one order of magnitude, from the cross-section to the surface;
- (ii) nanohardness and Young's modulus grow from the inner to the outer side for the Gastropoda *Conus mediterraneus* and Bivalvia *Pinna nobilis* shells, but an opposite trend is found for the Pecten *jacobaeus* and Venus *verrucosa* Bivalvia shells;
- (iii) no sensible difference has been observed as regards to the nanoindentation depth, with the exception of the softer inner anisotropic layer of the Gastropoda *Conus mediterraneus*, for which we have statistically deduced a volume-dominated dislocation sliding. This suggests a natural evolution against external attacks, from outside for the first two shells or during the "open" critical phase for the last two Bivalvia shells.

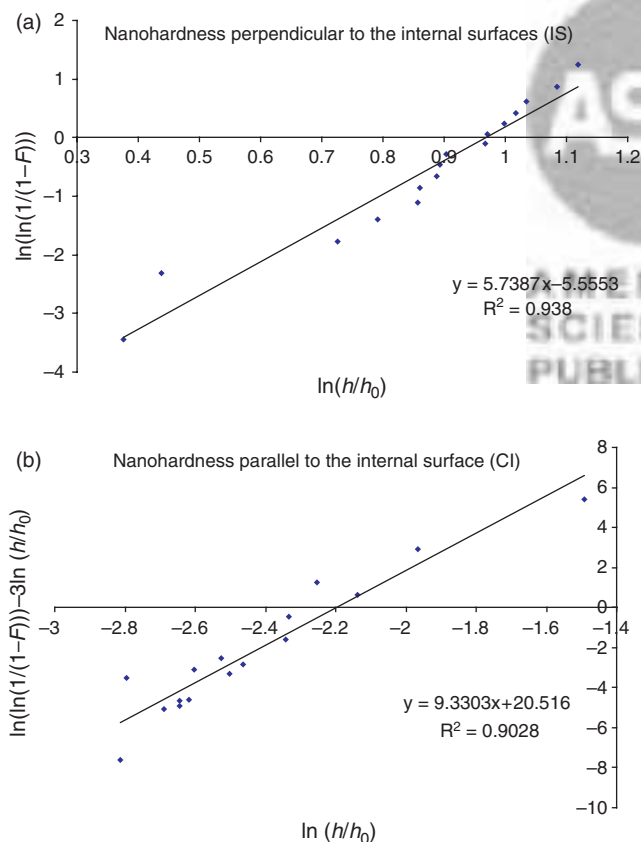


Fig. 7. (a) Statistical data analysis on nanohardness measured on the inner surface of the *Conus Mediterraneus* shell ($n = 0$). (b) Statistical data analysis on nanohardness measured on the cross section of the inner surface of the *Conus Mediterraneus* shell ($n = 3$).

Acknowledgments: Nicola M. Pugno acknowledges the financial support from the Piemonte

Region, “Converging Technologies,” Biotechnology–Nanotechnology, METREGEN 2008, “Metrology on a cellular and macromolecular scale for regenerative medicine.”

References and Notes

1. S. Kamat, H. Kessler, R. Ballarini, M. Nassirou, and A. H. Heuer, *Acta Mater.* **52**, 2395 (2004).
2. A. Y. M. Lin, M. A. Meyers, and K. S. Vecchio, *Mater. Sci. Eng., C* **26**, 1380 (2006).
3. R. Menig, M. H. Meyers, M. A. Meyers, and K. S. Vecchio, *Mater. Sci. Eng., A* **297**, 203 (2001).
4. D. F. Hou, G. S. Zhou, and M. Zheng, *Biomaterials* **25**, 751 (2004).
5. C. Linnæus, *Systema naturæ per regna tria naturæ, secundum classes, ordines, genera, species, cum characteribus, differentiis, synonymis, locis*, Tomus I, Editio Decima, Reformata, 10th edn., Holmiæ (Stockholm), (Laurentii Salvii) (1758).
6. J. G. Bruguère and C. H. Hwass, *Encyc. Méth. Hist. Nat. des Vers.* **2**, 690 (1792).
7. W. C. Oliver and G. M. Pharr, *J. Mater. Res.* **7**, 1564 (1992).
8. W. Weibull, *J. Appl. Mech.* **18**, 293 (1951).
9. N. Pugno and R. Ruoff, *J. Appl. Phys.* **99**, 024301 (2006).
10. C. Bignardi, M. Petraroli, and N. M. Pugno, *The Nanomechanics in Italy*, edited by N. M. Pugno, Research Signpost, Kerala, India (2007), p. 125.
11. N. Pugno, *Nanotechnology* **17**, 5480 (2006).
12. N. Pugno, *Int. J. of Fracture* **140**, 159 (2006).
13. M. Ippolito, A. Mattoni, L. Colombo, and N. Pugno, *Phys. Rev. B* **73**, 104111-1 (2006).
14. N. Pugno, B. Peng, and H. D. Espinosa, *Int. J. of Solids and Structures* **42**, 647 (2004).
15. A. Carpinteri and N. Pugno, *Powder Technology* **131**, 93 (2003).
16. A. Carpinteri, F. Ciola, and N. Pugno, *Computers and Structures* **79**, 389 (2001).

Received: 7 July 2009. Accepted: 22 September 2009.

Delivered by Ingenta to:
Rice University, Fondren Library
IP : 168.7.127.7
Mon, 06 Sep 2010 11:31:47

